NJC

PAPER

View Article Online
View Journal | View Issue

Cite this: *New J. Chem.*, 2017, **41**, 1526

Synthesis, metal binding and spectral properties of novel bis-1,3-diketone calix[4]arenes†

Sergey N. Podyachev,*[a] Svetlana N. Sudakova,[a] Gulnaz Sh. Gimazetdinova,[b] Nataliya A. Shamsutdinova,[a] Victor V. Syakaev,[a] Tatjiana A. Barsukova,[a] Nobuhiko Iki,[c] Dmitry V. Lapaev[d] and Asiya R. Mustafina[a]

Received 27th October 2016,
Accepted 10th January 2017

DOI: 10.1039/c6nj03381d

www.rsc.org/njc

New bis-1,3-diketone derivatives of calix[4]arene (**3–5**) have been synthesized with good yields by the addition of a sodium salt of acetylacetone, 1-benzoylacetone and dibenzoylmethane to 5,17-bis-(bromomethyl)-25,26,27,28-tetrahydroxycalix[4]arenes. The structural properties of the obtained compounds and their complexes have been established by means of IR, UV-Vis, NMR spectroscopy and quantum-chemical calculations. The complex ability of bis-1,3-diketones towards Al^{3+}, Ni^{2+}, Cu^{2+} and lanthanide ions (Nd^{3+}, Eu^{3+}, Tb^{3+}) has been investigated by using a liquid–liquid extraction method. The UV-Vis data indicate thermodynamically favorable 1 : 1 complex formation of the ligands with Tb^{3+} in alkaline DMF, although the time required for the equilibration reveals the difference between calix[4]arenes bearing acetylaceton-, benzoylaceton- and dibenzoylmethane-substituents. The steric hindrance effect on keto–enol transformation is the reason for the difference. The ligand-centered emissions of Gd^{3+} complexes with benzoylaceton- and acetylaceton-substituted calix[4]arenes reveal them both as more convenient antennae for red and infra-red than for green lanthanide luminescence. Indeed, the benzoylaceton-substituted counterpart sensitizes Yb^{3+}-centered luminescence to a good extent. Nevertheless, the luminescence of Tb^{3+} is sensitized by the acetylaceton-substituted counterpart to a better extent than that of Yb^{3+}, while only poor red Eu^{3+} emission is observed under sensitization by both the ligands.

1. Introduction

Among various functional building blocks, 1,3-diketones have found wide applications as key reagents for the design of a variety of organic compounds[1,2] and the synthesis of some drug compounds.[3] Moreover, 1,3-diketone derivatives are known as invaluable chelating ligands for many transition metals in materials chemistry[3–6] and can be potentially used in the synthesis of extractants[6] and luminescent materials.[7–11] Luminescent lanthanide complexes attract much attention due to their usage in optical communications and solar energy conversion,[12–15] as well as in fluoroimmunoassay, bio-medical diagnostics and therapy.[16–20] It has been well demonstrated that 1,3-diketones are ideal candidates for the sensitization of visible and near infrared (NIR) luminescence emitted by lanthanide ions due to the significant antenna effect. The introduction of bulky and fluoro-aliphatic substituents into 1,3-diketones can significantly improve lanthanide luminescence.[11,21] Therefore, the design and synthesis of new 1,3-diketone ligands bearing various substituents seems to be an exciting topic of current investigations.

Anchoring of functional groups on the suitable molecular platforms is worth noting as a promising strategy for preparing more advanced ligands with improved binding efficiency and selectivity towards metal ions. This tendency has become a challenging factor for the synthesis of poly-1,3-diketones.[5,22,23]

Recently, we have shown[24,25] that calix[4]arenes and calix[4]-resorcines serve as very promising platforms for embedding four 1,3-diketone moieties. The synthesized compounds appeared to be a rather effective antennae for Tb(III)-centered luminescence. The hydrophilic colloids prepared on the basis of Tb(III) and Gd(III) tetra-1,3-diketonate complexes were found to be promising candidates for biomedical applications as contrast agents due to their high photophysical[24] and magnetic relaxation[26] parameters correspondingly.

Despite the presence of four 1,3-diketone groups at the upper rim of the above mentioned calix[4]arenes, the coordination with metal ions was realized only by means of two chelating groups of one molecule, which favors further formation of a

[a] *A. E. Arbuzov Institute of Organic and Physical Chemistry, Kazan Scientific Center of Russian Academy of Sciences, Arbuzov str., 8, 420088, Kazan, Russia. E-mail: spodyachev@iopc.ru; Fax: +7-843-273-1872*
[b] *Kazan National Research Technological University, K. Marks str., 68, 420015, Kazan, Russia*
[c] *Graduate School of Environmental Studies, Tohoku University, 6-6-07 Aramaki-Aoba, Aoba-ku, Sendai 980-8579, Japan*
[d] *Zavoisky Physical-Technical Institute of Kazan Scientific Center of Russian Academy of Sciences, 420029 Kazan, Russia*

† Electronic supplementary information (ESI) available. See DOI: 10.1039/c6nj03381d

ternary complex. This fact is obviously the main reason for the luminescence response and realization of a sensing function of polyelectrolyte-coated colloids based on Tb(III) complexes of the calix[4]resorcinarene cavitand towards some of substrates in aqueous solutions.[27] From this point of view, the synthesis of bis-1,3-diketone derivatives based on the calix[4]arene platform is an attractive direction in the design of lanthanide complexes for bio- and chemosensing. It is also worth noting that embedding aromatic substituents to ligands is a widely applied route to enhance the antenna-effect of the ligand and/or to make the ligand more suitable for sensitizing red or near infra-red lanthanide-centered luminescence.

Thus, herein, we report the synthesis of new bis-1,3-diketone derivatives of calix[4]arene bearing methyl and phenyl terminal substituents in 1,3-diketone fragments. The lipophilicity of calix[4]arene derivatives is the prerequisite for studying them in liquid–liquid extraction of some metal ions (Al^{3+}, Ni^{2+}, Cu^{2+}, Nd^{3+}, Eu^{3+}, and Tb^{3+}). The spectroscopic properties of the new calix[4]arene derivatives and the luminescence behaviour of their Tb^{3+}, Gd^{3+}, Eu^{3+} and Yb^{3+} complexes have been considered and compared with the previously obtained data for the tetra-1,3-acetylacetonyl analogue with an aim to highlight structure impact in complex ability and the antenna effect of novel compounds.

2. Results and discussion

2.1. Synthesis and characterization of bis-1,3-diketone calix[4]arenes 3–5

The synthetic procedures for the series of bis-1,3-diketones are summarized in Scheme 1. The halogenmethylated derivatives of calix[4]arenes can be successfully applied for the anchoring of 1,3-diketone groups at the upper rim of calix[4]arenes. In the case of tetra-hydroxy substituted calix[4]arenes, the halogenmethylation is carried out in the presence of an excess of alkyl chloromethyl ether and tin tetrachloride.[28] The calix[4]arenes can be also chloromethylated by using paraformaldehyde/HCl in a dioxane/H_3PO_4/AcOH mixture.[29–31] The synthesis of tetrahydroxy-tetrakis(halogenmethyl)calix[4]arene was previously performed by the interaction of **1** with an excess of paraformaldehyde in the presence of Zn and HBr in glacial acetic acid.[32] It was recently demonstrated that this reaction can be also applied for obtaining bis-halogen derivatives of the calix[4]arene **2**.[33] We have successfully synthesized compound **2** by using a slightly modified literature procedure. The reaction was carried out at room temperature for 5 days in the presence of 3 equivalents of paraformaldehyde. The spectral parameters of the obtained product **2** are in full agreement with the literature data.[33]

The synthesis of bis-1,3-diketone derivatives was fulfilled by the addition of a sodium salt of the corresponding 1,3-diketone to the 5,17-bis-(bromomethyl)-25,26,27,28-tetrahydroxycalix[4]arene **2** in anhydrous dioxane under vigorous stirring. It should be noted that in all cases, the addition of sodium salt was accompanied by an intense pink-violet color which gradually changed to brownish yellow. A similar phenomenon was previously reported for tetra-substituted analogue **6**.[25] This color can be obviously explained by the formation of intermediate quinone structures in the reaction mixture after addition of a basic salt to compound **2**.[34,35] A high reactability of this intermediate brought about the target bis-1,3-diketones **3–5** with good yields (52–60%) even without heating. The obtained novel compounds were characterized by IR, ^{1}H NMR, ^{13}C NMR and MALDI-MS techniques.

The presence of a more broadened absorption band at $\sim$1600 cm^{-1} in the IR spectrum of compound **3** in comparison with **4** and **5** is probably caused by a considerable amount of the enol form in the former compound. The strong hydrogen bonding of the lower rim hydroxyl groups for **3–5** is evident from broadened and intensive bands ν(OH) at $\sim$3160–3193 cm^{-1} that are substantially lower than $\nu(OH)_{free}$ $\sim$3500–3600 cm^{-1}.[36]

Assignment of the signals in the NMR spectra of **3–5** (Table 1) was accomplished by means of 2D COSY, ^{1}H–^{13}C HSQC and ^{1}H–^{13}C HMBC experiments. It is well known that 1,3-diketones can exist as keto–enol tautomers.[37] In the case of the bis-1,3-diketones, three main equilibrium forms can be realized (Scheme 2). According to ^{1}H NMR data, the content of the enol form in $CDCl_3$ solution amounts to 39% for **3** (C_3 = 30 mM), which leads to the appearance of an additional set of signals in the NMR spectra of the compound. However, it is difficult to estimate the contribution of each form because of overlapping

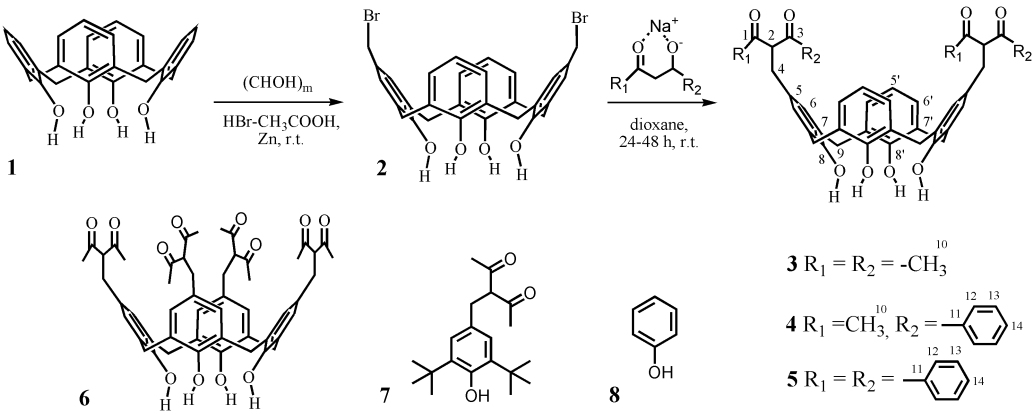

Scheme 1 Synthetic routes and structural formulae of the investigated compounds **1–8**. A similar numbering system of atoms is used in Table 1.

Table 1 ^{1}H and ^{13}C chemical shifts[a] (ppm) and spin–spin coupling constants (Hz) observed for the keto form[b] of calix[4]arenes **3–5** in $CDCl_3$

	Compound					
	3		**4**		**5**	
Atom	^{1}H	^{13}C	^{1}H	^{13}C	^{1}H	^{13}C
1	(16.80–16.83(OH))	203.6 (192.0)	(17.05(OH))	203.3	(17.1–17.3(OH))	195.7
2	3.89	70.3 (108.5)	4.69	65.0	5.40 t, ^{3}J = 6.7	59.2
3				196.2		
4	2.91 (3.43)	34.2 (32.08)	3.10	34.2	3.19 d, ^{3}J = 6.7	44.6
5		131.9 (135.1)		132.2		132.8
5′	6.77 t, ^{3}J = 7.3	129.4	6.74 t, ^{3}J = 7.6	122.4	6.74 tr, ^{3}J = 7.5	122.4
6	6.76 (6.71)	128.4 (122.4)	6.83	129.5	6.87	129.7
6′	7.03 d, ^{3}J = 7.3	129.2	7.07 d, ^{3}J = 7.6	129.2	7.07 d, ^{3}J = 7.5	129.2
7		128.0 (127.9)		128.5		128.5
7′		122.4				128.4
8	10.0–10.3	149.0 (147.4)	10.2 (OH)	149.0	10.07 (OH)	147.5
8′		147.7		147.5	10.20 (OH)	149.0
9	3.41 eq.	31.9	3.37 eq.	31.8	3.33 eq. d, ^{2}J = 13.9	31.7
	4.17 ax.		4.11 ax		4.07 ax. d, ^{2}J = 13.9	
10	2.10 (2.00)		2.10	28.82		
11				136.6		136.1
12			7.78	128.7	7.77 d, ^{3}J = 7.6	128.6
13			7.22	128.8	7.20 t, ^{3}J = 7.6	128.9
14			7.34	133.8	7.33 t, ^{3}J = 7.6	133.6

[a] Numbering according to Scheme 1. [b] The assignment for the enolic forms is given in parentheses.

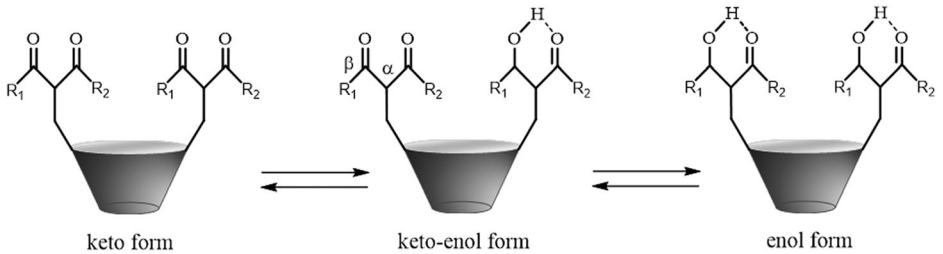

Scheme 2 Keto–enol tautomerization of bis-1,3-diketone calix[4]arenes.

of the signals. In the case of **4** and **5**, the enol form content is negligible (<0.1% for $C_{3,4}$ = 30 mM).

Hydrogen atoms in the enol fragments participate in the formation of strong hydrogen bonds (δ ^{1}H(OH) = 16.80–16.83 ppm for **3**). It is interesting to note that the amount of the enol form realized in compound **3** is almost the same as in tetra-1,3-diketone **6** (40%).[25] This fact testifies a weak mutual influence of 1,3-diketone groups on the keto–enol tautomerism in the investigated calix[4]arene derivatives. It can be also supposed that the substitutents in these compounds are turned out from the calix[4]arene cavity.

For all synthesized compounds **3–5** only a single peak of methylene-bridged carbon atoms is detected, which indicates a cone or a 1,3-alternate isomer of calix[4]arenes. According to the ''de Mendoza rule'',[38] the determined values of chemical shifts for these atoms ((δ ^{13}C(9) = 31.9 ppm for **3**, 31.8 ppm for **4** and 31.7 ppm for **5**) testify undoubtedly the cone isomer form for all investigated calix[4]arenes.

The chemical shifts for hydroxyl protons localized at the low rim of calix[4]arene molecules are not practically changed on going from parent calix[4]arene **1** (10.19 ppm)[39] to the calix[4]arenes **3–5** (δ ^{1}H(8) = 10.0–10.3 ppm). These data indicate the maintenance of the initial cone conformation for calix[4]arene derivatives **3–5**, stabilized by a circular hydrogen bond between hydroxyl groups similar to the calix[4]arene **1**.[40]

2.2. Extraction of metal ions by bis-1,3-diketones 3–5

As it was mentioned above, 1,3-diketones are invaluable chelating ligands for complex formation with various transition metal ions and thus can extract metal ions from an aqueous phase to an immiscible organic phase. However, the application of more simple representatives of 1,3-diketones, such as acetylacetone or 1-benzoylacetone, is rather complicated due to the fact that their metal complexes are too hydrophilic to allow extraction into a nonpolar organic phase.[6] Therefore, fixing of 1,3-diketone chelating groups on the calix[4]arene platform should be a very promising way to gain hydrophobicity and water insolubility, which can contribute to further development of extracting agents.

The extractability of new bis-1,3-diketone calix[4]arenes **3–5** towards some industrially critical metal ions such as Al^{3+}, Ni^{2+}, Cu^{2+} and rare-earth ions (Nd^{3+}, Eu^{3+}, Tb^{3+}) was estimated by the competitive extraction of the cations from their aqueous mixture into chloroform. The extraction was carried out during 24 hours to reach equilibrium conditions. The results shown in

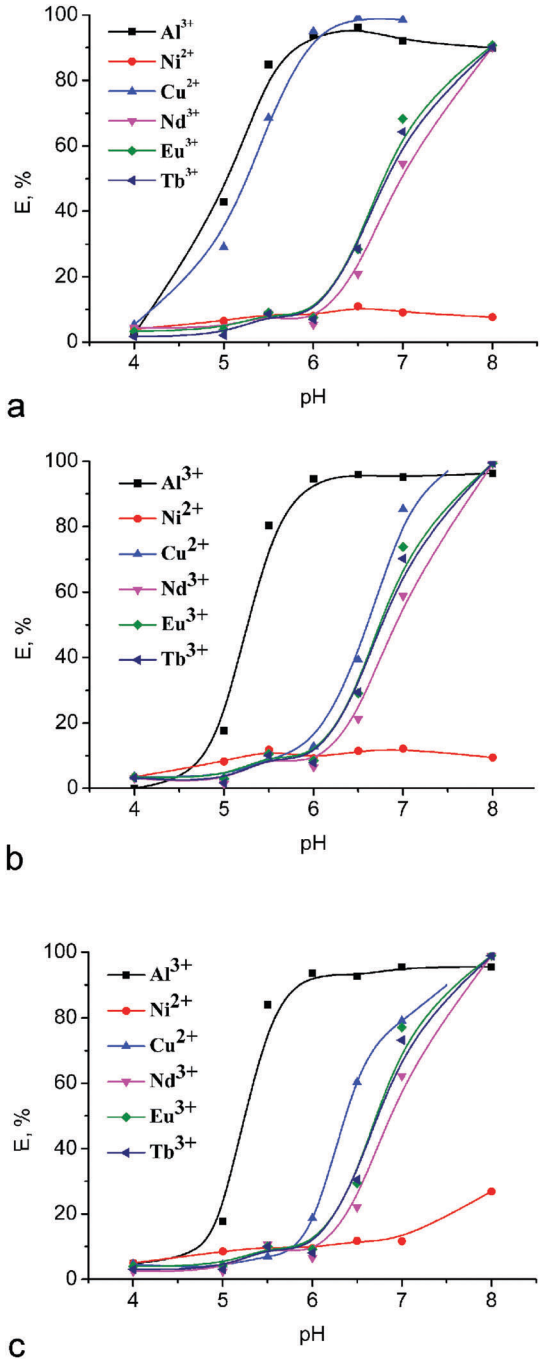

Fig. 1 Effect of pH on the extraction percentage for different metal ions with (a) **3**, (b) **4** and (c) **5**. [Metal ion] = 0.1 mM; [L_{3-5}] = 0.5 mM.

Fig. 1 demonstrate that the extraction percentage for metal ions goes up on going to higher pH, which can be explained by easier ionization of 1,3-diketone groups under alkaline conditions and hereby testifies that these cations are extracted due to the ion-exchange process.

In the case of bis-1,3-acetylacetonyl derivative **3**, notable extraction of Al^{3+} and Cu^{2+} was detected after pH 4.0, but Nd^{3+}, Eu^{3+} and Tb^{3+} metal ions were extracted by this compound only at pH > 6. An almost quantitative extraction (>90%) for the former metal ions was already observed at pH 6, while the extraction of lanthanide ions reached a maximum at pH 8. At the same time, a quite low extractability of the derivative **3** towards Ni^{2+} ions (E < 11%) was observed in the whole range of pH values. In the case of bis-1,3-diketones **4** and **5**, the extraction of Al^{3+} and Cu^{2+} was detected only after pH 5 and 6, which is obviously due to the lower acidity of these compounds in comparison with **3**. The results obtained earlier for the acidity of tris(1,3-diketones) having similar substitutents and linked by the mesitylene spacer support this assumption.[41] However, the extraction of lanthanide ions by compounds **4** and **5** also begins after pH 6 and becomes quantitative at pH 8, as well as for **3**. The extraction efficiency for the investigated bis-1,3-diketones **3–5** remains the same and depends only slightly on the nature of the lanthanide ion.

It is worth noting that the presence of hydroxyl groups at the low rim of calix[4]arene molecules makes their participation in the coordination of metal ions possible. It was established, however, that the unmodified "classical" *p-tert*-butylcalix[4]arene only scarcely extracts transition metal ions (E% for Ni^{2+} and Cu^{2+} ~1%) under similar experimental conditions.[42] Therefore, a main role in the binding of metal ions by compounds **3–5** belongs to 1,3-diketone groups fixed at the upper rim of the calix[4]arene backbone.

Thus, we have shown here that bis-1,3-diketone calix[4]arenes **3–5** can act as rather effective pH-dependent extraction agents. The selective extraction of Cu^{2+} *versus* Ni^{2+} can be utilized for analytical purposes. The lack of selectivity in the extraction of Nd^{3+}, Eu^{3+}, and Tb^{3+} reveals **3–5** as group extractants for lanthanide ions.

2.3. Electronic absorption spectroscopy

UV-Vis spectroscopy is a powerful tool to study complex formation of 1,3-diketones with lanthanide ions. This method is of particular importance for 1,3-diketone derivatives of calix[4]arenes and calix[4]resorcinarenes, since phenol and resorcinol moieties significantly contribute to the spectral behavior of their derivatives.[24,25] The UV-Vis absorption spectra of the calix[4]arenes **1**, **3–6**, model compound **7** as well as phenol **8** recorded in DMF are shown in Fig. 2 and 3. Spectroscopic data are summarized in Table 2.

The absorption spectra of the investigated compounds demonstrate rather high values of the molar extinction coefficients (ε_{max} = 8.83 × 10^3 M^{-1} cm^{-1} to 20.81 × 10^3 M^{-1} cm^{-1}) with λ_{max} in the range of 275 nm to 292 nm (Table 2) typical for π–π* electron transitions. Additionally, it is worth noting the shoulders at 310–340 nm in the spectra of the calix[4]arenes **3–5**. A comparison of UV–Vis spectra for the model compounds **7** and **8** and the calix[4]arene molecules indicates that the absorptions of phenol and 1,3-dikenone fragments incorporated on the calix[4]arene platform are practically independent and additive. This tendency can be exemplified by the ε_{max} values of phenol **8** (ε_{max} = 2.28 × 10^3 M^{-1} cm^{-1} at 274 nm) and calix[4]arene **1** (ε_{max} = 9.22 × 10^3 M^{-1} cm^{-1} at 275 nm). Similarly to this case, the absorption of bis-1,3-diketone **3** (ε_{max} = 13.42 × 10^3 M^{-1} cm^{-1}) can be approximated as the sum of the absorptions of its structural blocks (ε_{calc} = 2(ε_7 + ε_8) = 11.98 × 10^3 M^{-1} cm^{-1}). Such additivity indicates the lack of any

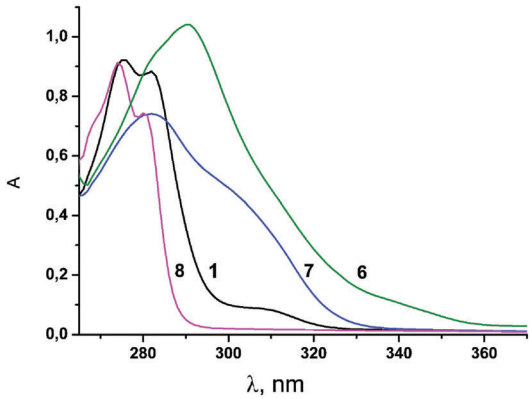

Fig. 2 UV-vis spectra of compounds **1**, and **6–8** in DMF solution (C_1 = 0.1 mM, C_6 = 0.05 mM, C_7 = 0.2 mM, C_8 = 0.4 mM).

conjugation between the chromophoric units of **3**. However, a rather noticeable bathochromic shift (~10 nm) is observed for **6** in comparison with **7**. The ε_{max} value for **6** (ε_{max} (292 nm) = 20.81 × 10^3 M^{-1} cm^{-1}) also deviates from ε_{calc} ($\varepsilon_{calc} = 4\varepsilon_7$ = 14.84 × 10^3 M^{-1} cm^{-1}). This result points to an impact of intramolecular interactions between four 1,3-diketone substitutents fixed on the macrocyclic platform on the spatial structure and spectral behavior of **6**.

UV-Vis spectroscopy was applied to reveal the complex formation properties of ligands **3–5**. The spectral changes of **3** under its complex formation with Tb(III) (Fig. 3a) are similar to those previously reported for its tetra-1,3-diketone counterpart **6**.[25] The spectral changes of **4** (Fig. 3b) are much less pronounced than those of **3** immediately after sample preparation, and tend to increase with time on approaching the equilibrium conditions in three days. A new intensive maximum at ~320 nm appears in the spectrum of **4** when equilibrium conditions are attained. The time dependence for ligand **5** is more pronounced than that for **4** (Fig. S1, ESI†). In particular, insignificant spectral changes of **5** are observed within one day after the admixture of Tb^{3+} and TEA. Moreover, four days of storage of the solutions is not obviously enough for the achievement of equilibrium conditions for **5** (Fig. S1, ESI†). Moreover, the appearance of a new absorption band at about 350 nm in alkalized DMF solutions of calix[4]arene **5** and Tb^{3+} salt (Fig. 3c) is another difference between **5** and **4**. The reasons for the time consuming complex formation are worth discussing.

Literature data highlight keto–enol tautomeric transformation as the most time-consuming step in complex formation, which is greatly affected by the substituent effect[37,43,44] and nature of the solvent.[37,45] It is worth noting that the α-substituent effect (α-position is designated in Scheme 2) is well documented in the literature,[37,46] although no significant retardation of keto–enol transformation is observed for **3** (Fig. S1, ESI†) and its tetrakis-1,3-diketone counterpart,[25] where acetylacetone moieties are fixed at the calix[4]arene backbone through α-substitution by a methylene linker. Nevertheless, in the case of the tetrakis-[(1,3-acetylaceton-3-yl)] derivative of calix[4]resorcine cavitand, which possesses a rather more rigid conformational structure, time dependent complex formation was observed.[24]

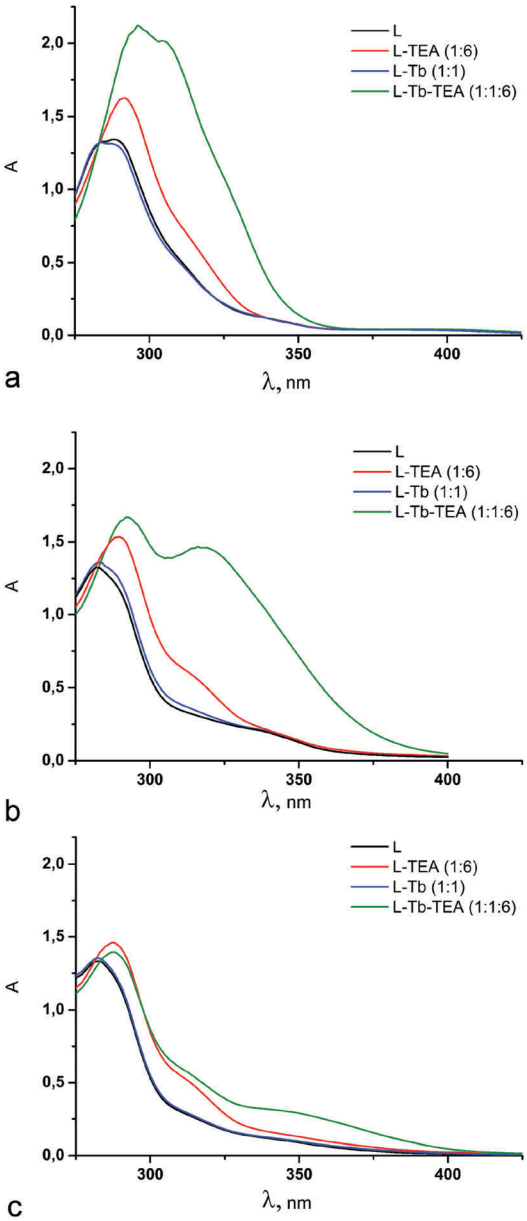

Fig. 3 UV-Vis spectra of **L** (**3** (a), **4** (b) and **5** (c)) (C_L = 0.1 mM) in DMF (L); **L** in alkalized DMF (C_{TEA} = 0.6 mM) (L-TEA (1 : 6)); **L** with $Tb(NO_3)_3$ (C_{Tb}^{3+} = 0.1 mM) (L-Tb (1 : 1)), and **L** with $Tb(NO_3)_3$ in alkalized DMF (L-Tb-TEA (1 : 1 : 6)). The spectra were recorded under equilibrium conditions.

Table 2 UV-Vis spectral data for compounds **1**, and **3–8**

Compound	λ_{max} (nm)	ε_{max} (10^3 M^{-1} cm^{-1})	Compound	λ_{max} (nm)	ε_{max} (10^3 M^{-1} cm^{-1})
1	275	9.22	**6**	292	20.81
	282	8.83			
3	288	13.42	**7**	282	3.71
4	282	13.25	**8**	274	2.28
				280	1.86
5	283	13.33			

Some differences between keto–enol tautomeric transformations under substitution of methyl-groups of acetylacetone to

phenyl moieties in dibenzoylmethane are highlighted in the literature,[47] although they cannot explain the above mentioned difference in the complex formation for **3** and **5**. Thus, the observed tendency points to the impact of both α- and β-substituents on the keto–enol tautomerism of 1,3-diketone derivatives of calix[4]arenes **3–5** under alkaline conditions. The above mentioned ^{1}H NMR data also reveal the insignificant contribution of the enolic form for **4** and **5** in $CDCl_3$, while both forms of **3** are in equilibrium under similar conditions.

The stabilization of the enolic form in non-polar solvents is well documented.[37] On the other hand, the hydration is worth noting as another factor shifting the keto–enol equilibrium.[41] These factors explain the lack of a detectable difference in the complex formation behavior of compounds **3–5** at the water–$CHCl_3$ interface after 24 hour exposition (Fig. 1). This result indicates that the difference in keto–enol tautomerization for **3–5** is negligible in the extraction process conditions due to a greater rate of keto–enol transformation in the biphasic system.

In order to evaluate the stoichiometry of complex formation, a Job plot analysis of the spectral measurements with a varied L : Tb^{3+} molar ratio and a constant L : TEA molar ratio in DMF solutions has been performed. It can be clearly seen from Fig. 4 that in all cases, the long-term storage of DMF solutions containing Tb^{3+} complexes of the investigated ligands **3**, **4** and **5** results in the maximum in the Job's plot being at 0.5 molar ratio. This fact apparently indicates that the Tb^{3+} ion preferably forms complexes of 1 : 1 stoichiometry with these compounds. It should be also noticed that at the initial stage, complexes of n : 1 ($n > 1$) stoichiometry are obviously accumulated, which is well demonstrated in Fig. 4b for the ligand **4** after one day of solution storage (maximal L : Tb^{3+} ratio at 0.67). The observed tendency points to the transformation of kinetically favorable complexes of n : 1 stoichiometry into more thermodynamically stable 1 : 1 complexes after more prolonged time of storage (3 days).

To confirm the assumed stoichiometry of the thermodynamically stable complexes we have accomplished a spectral titration experiment for compounds **3–5** with 1 : 1 molar ratio of Tb : L and varied L : TEA molar ratio in DMF solutions (Fig. 5). The obtained data testify that the addition of an excess of TEA leads to the deprotonation of two diketone groups from the molecule of bis-1,3-diketone **3** (Fig. 5a). Only one proton is eliminated in Tb(III)-containing alkaline solutions of **4** and **5** after one day of storage, while storage for four days at least is required for the second proton elimination (Fig. 5b and c). The results indicate 1 : 1 complex formation of Tb^{3+} *via* two deprotonated 1,3-diketone groups. Additionally, quantum-chemical calculations have been accomplished to confirm the probability of this coordination mode.

2.4. The quantum-chemical calculations

Our previous report[25] highlighted that only two 1,3-diketonate groups of **6** participate in the coordination of one lanthanide ion. Moreover, efficient coordination of lanthanide ions can be realized for all possible conformations of the calix[4]arene backbone. This fact is of particular importance under alkaline conditions, where deprotonation of the phenolic lower rim is the reason for conformation shift from cone to 1,2- or 1,3-alternates.

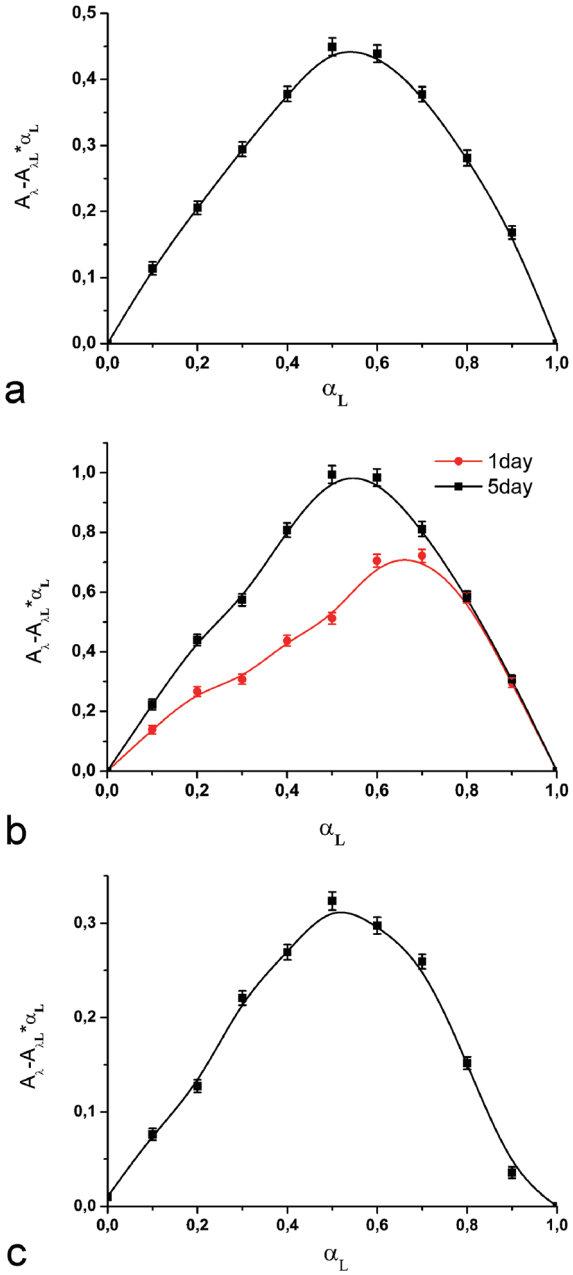

Fig. 4 The Job plot profiles of DMF solutions at varied L : Tb^{3+} molar ratios: (a) λ = 320 nm, [Tb^{3+}] + [**3**] = 0.1 mM, L : TEA (1 : 6) and time of solution storage 1 day; (b) λ = 320 nm, [Tb^{3+}] + [**4**] = 0.2 mM, L : TEA (1 : 6) and times of solution storage 1 day and 5 days; (c) λ = 340 nm, [Tb^{3+}] + [**5**] = 0.2 mM, L : TEA (1 : 10) and time of solution storage 5 days.

Taking into account these tendencies, the efficiency of coordination of bis-1,3-diketone-derivatives **3–5** with lanthanide ions also can be realized in different conformations of the calix[4]arene backbone, including cone, partial cone and 1,3-alternate.

Relative heat of formations for conformers of calix[4]arene **3** and their complexes [$Tb^{3+}L^{n-}$] were obtained using MOPAC 2012 (Table 3). The structures obtained after SPARKLE/PM7 optimizations are presented in Fig. 6. The theoretically predicted stability order for **3** is cone > partial cone > 1,3-alternate (Table 3), which correlates with the number of hydrogen bonds between

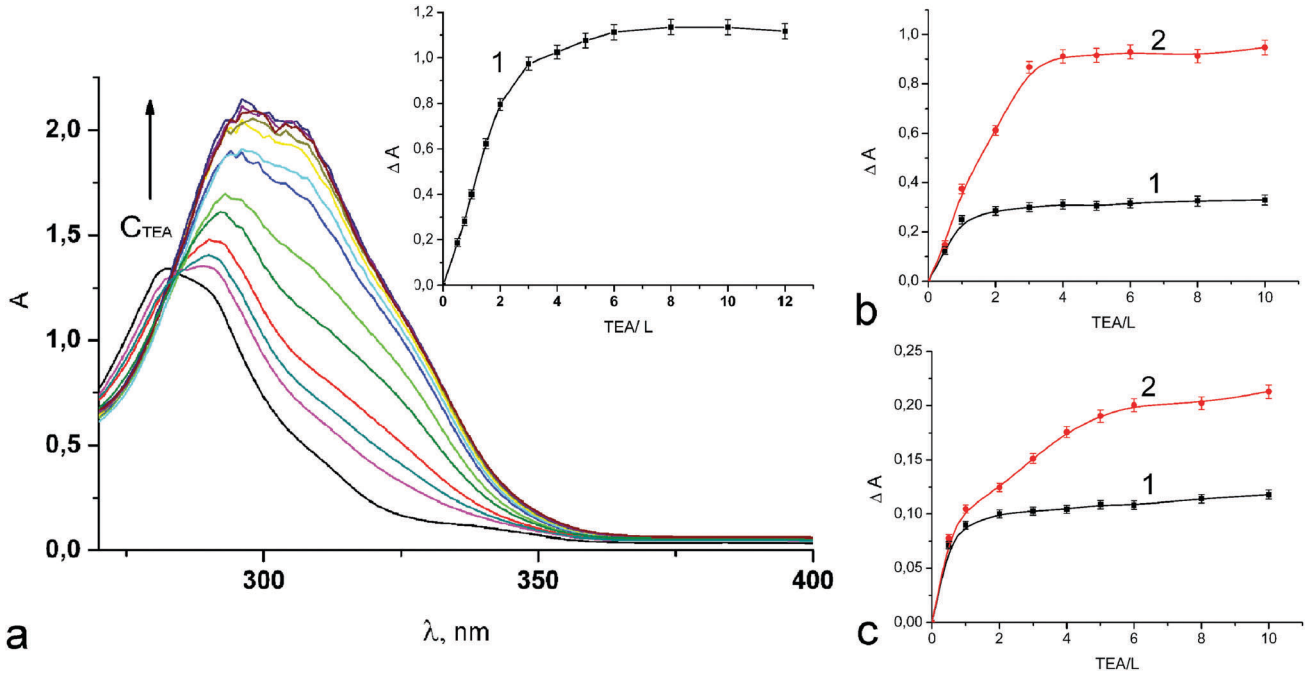

Fig. 5 UV-Vis spectra and ΔA (λ = 320 nm) of the DMF solutions of **3** (a), **4** (b) and **5** (c) with $Tb(NO_3)_3$ ([**3**] = [**4**] = [**5**] = [Tb^{3+}] = 0.1 mM) at varied TEA : L molar ratios and time of solution storage 1 day (1) and 4 days (2).

Table 3 Relative heat of formations calculated for conformers of calix[4]arene **3** and its complexes [$Tb^{3+}L^{n-}$]

	ΔH°_{298} (kcal mol^{-1})		
Compound	Cone	Partial cone	1,3-Alternate
L	0	17.38	22.48
[$Tb^{3+}L^{2-}$]	0	13.47	27.33
[$Tb^{3+}L^{3-}$]	0	13.69	29.37

the OH groups at the calix[4]arene lower rim. This tendency is in agreement with the previous reports about the same stability order for conformers of calix[4]arene without any upper-rim substituents.[48,49] The same tendency is revealed for Tb^{3+} complexes of **3**, where the most energy gain is in cone conformation. In particular, the cone conformer of **3** is most favorable for both [$Tb^{3+}L^{2-}$] and [$Tb^{3+}L^{3-}$], where two 1,3-diketone groups are deprotonated. It is also worth noting that deprotonation of the phenolic lower rim of calix[4]arene **3** insignificantly influences the energy gap between the conformers (Table 3).

2.5. Photoluminescence spectroscopy

UV-Vis spectral data reveal similarity in complex formation for bis-(**3**) and tetrakis-1,3-diketone **6**, which is confirmed by the similarity in the spectra of Tb^{3+}-centered steady-state luminescence for the Tb^{3+} complexes of **3** and **6** (Fig. 7a, corresponding excitation spectra are shown in Fig. S2a, ESI†). At the same time, the sensitizing effects of ligands **4** and **5** on Tb^{3+}-centered luminescence are insignificant. The steady state spectra point to some difference in the antenna-effects of ligands **3** and **6** on Tb^{3+}-centered luminescence.

The time-resolved luminescence measurements (see Fig. S3 in the ESI†) reveal the longer excited state lifetime for the Tb^{3+}-centered luminescence in complexes with ligand **3** (0.127 ± 0.004 ms) than that for its tetra-1,3-diketone counterpart **6** (0.053 ± 0.002 ms). This fact confirms coordination of Tb^{3+} ions by 1,3-diketonate groups of **3** as the dominant coordination mode under alkaline conditions (see Fig. 6). The longer lifetime of the Tb(III) complex with **3** compared with **6** points to either less non-radiative de-activation or less back transfer, or both. The interfering effect of 1,3-diketone groups of **6** not participating in coordination with Tb^{3+} ions can be assumed as a reason for more energy stock from the excited Tb^{3+} state to the vibrational levels of the ligand in comparison with **3**. It is worth noting that the above mentioned peculiarity in the spectral behavior of **6**, which is a bathochromic shift and adsorption non-additivity (see Section 2.3), correlates with the interfering effect of four 1,3-diketone groups embedded to the calix[4]arene backbone.

Literature results highlight the effect of aromatic or aliphatic substituents in 1,3-diketones on both the energy of singlet and triplet excited state levels and the intersystem crossing, which in turn affects their ability to sensitize lanthanide-centered luminescence.[50] Dibenzoylmethane is well documented for its good antenna effect on near infra-red lanthanide-centered luminescence.[51] Thus, Tb^{3+}-, Eu^{3+}- and Yb^{3+}-centered luminescence measured for 1 : 1 complexes of ligands **3**, **4**, **5** and **6** is presented in Fig. 7 along with ligand-centered luminescence of the Gd^{3+} complex with **3**–**5**. The corresponding excitation spectra are presented in Fig. S2 in the ESI.† The luminescence spectra of Gd(III) complexes are commonly applied in measuring the triplet level energy of the ligands in their lanthanide complexes due to Gd(III)-enhanced intersystem crossing.[52] The luminescence spectra of Gd(III) complexes presented in Fig. 7b were recorded

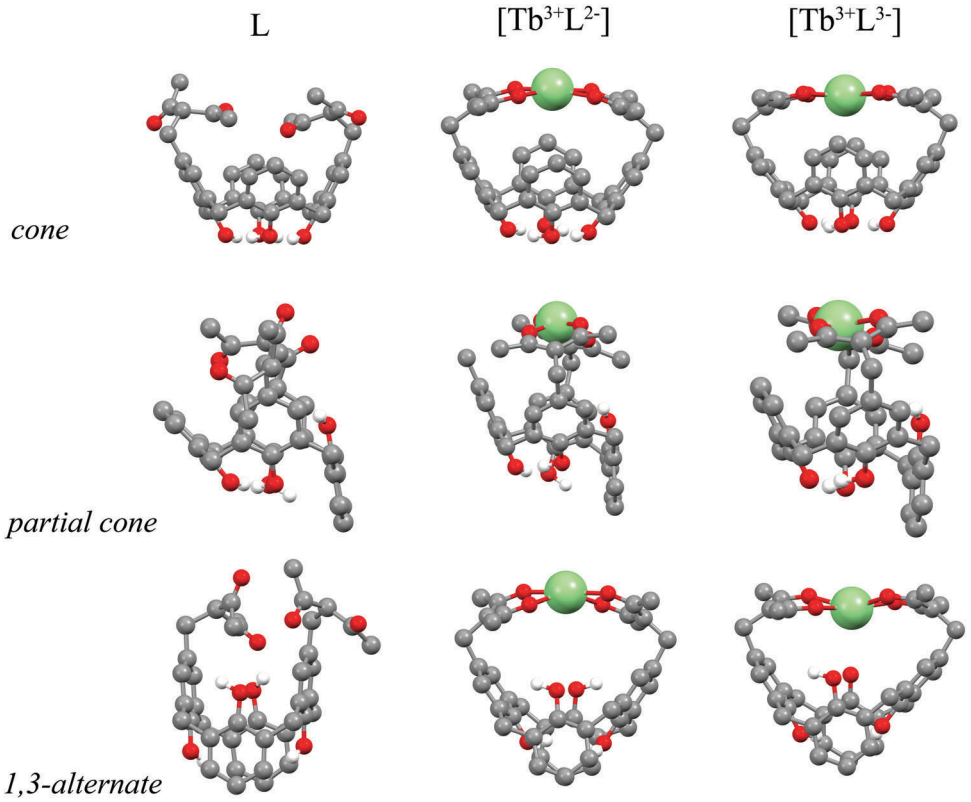

Fig. 6 Sparkle/PM7 model optimized structures of three conformers of **3** and their Tb^{3+} complexes. Hydrogen atoms are omitted for clarity with the exception of the phenolic hydrogens.

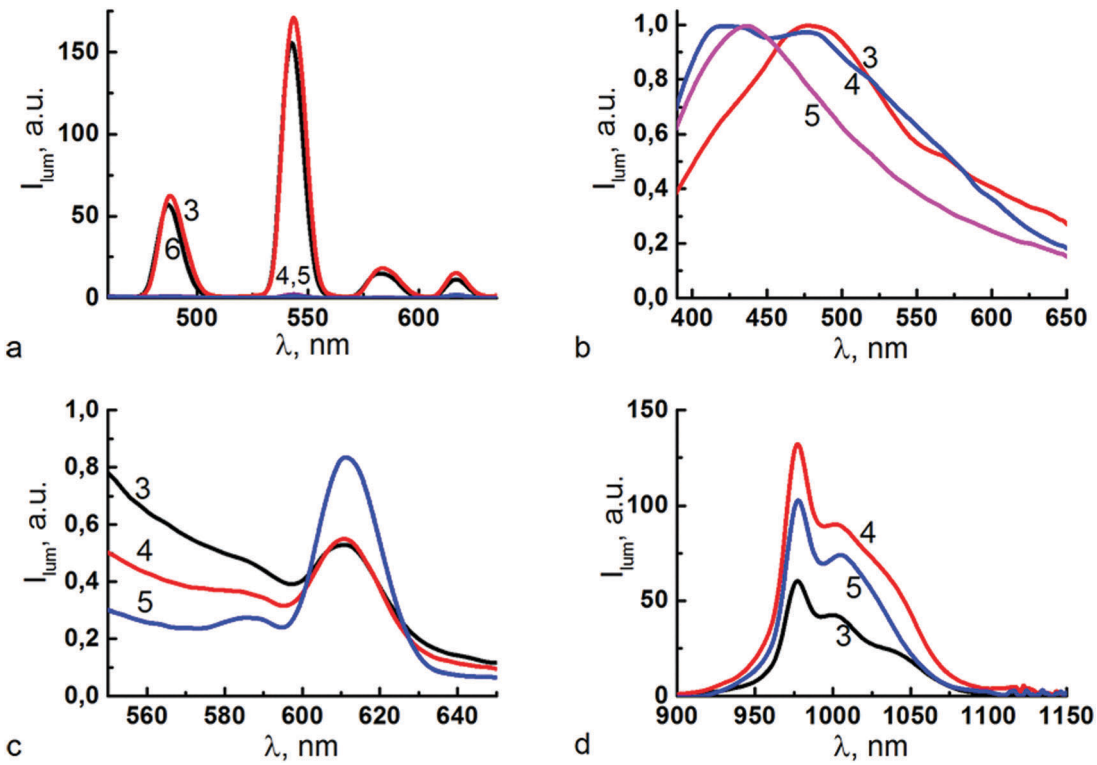

Fig. 7 Luminescence spectra of alkalized DMF solutions of ligands **L** = **3–5** with Ln^{3+} = Tb^{3+} (a); Gd^{3+} (b), Eu^{3+} (c) and Yb^{3+} (d). λ_{ex} = (a) 327 nm (**3**), 340 nm (**4** and **5**) and 330 nm (**6**); (b) 337 nm (**3–5**); (c) 345 nm (**3**), 340 nm (**4** and **5**); (d) 330 nm (**3**), 370 nm (**4** and **5**). (a and c) $C_L = C_{Ln^{3+}}$ = 0.1 mM, C_{TEA} = 0.4 mM. (b) $C_L = C_{Gd^{3+}}$ = 1 mM, C_{TEA} = 4 mM. (d) $C_L = C_{Yb^{3+}}$ = 0.2 mM, C_{TEA} = 0.8 mM. Ligands are designated in the spectra by corresponding numbers. Luminescence spectra of Gd(III) complexes were recorded with 20 μs delay time.

with a pronounced (20 μs) delay time in order to minimize the contribution of singlet level derived emission. Fig. S3 in the ESI† represents the ligand-centered luminescence for Gd(III) complexes recorded with the delay time varying within 1–20 μs.

The measured spectra indicate that Tb^{3+}-centered luminescence is the highest for the complexes with **3** *versus* those with **4** and **5** (Fig. 7a). The Eu^{3+}-centered luminescence is very weak for all measured complexes (Fig. 7c). The Yb^{3+}-centered luminescence is the highest for the complexes with **4** *versus* those with **5** and **3**. It is worth noting that the different kinetic conditions designated in the previous section were taken into account in the measurements of lanthanide-centered luminescence. Nevertheless, storage for three days is enough for the completed complex formation with lanthanides for **4**, while the complex formation is still incomplete for **5** under the same conditions. Thus, the data obtained for **5** is greatly affected by the kinetic retardation of complex formation, while the kinetic effect is negligible for **4**.

The luminescence spectra presented in Fig. 7a indicate that ligand **4** provides a worse antenna effect on Tb^{3+}-centered luminescence than **3** and **6**. The opposite tendency is observed for Yb^{3+}-centered luminescence (Fig. 7d), where ligand **4** sensitizes Yb^{3+} luminescence to a better extent than **3**, while rather weak emission bands at 614 nm are observed for Eu^{3+}-centered luminescence for all ligands. The spectral pattern of Yb^{3+} complexes (Fig. 7d) reveals emission at 976 nm, which corresponds to the 0-phonon component of the $^2F_{5/2} \rightarrow {}^2F_{7/2}$ transition with additional transitions at lower energy assigned to transitions to other crystal field sublevels of the ground state and/or to vibronic contribution. Thus, ligand **4** can be considered as an antenna for Yb^{3+}-centered NIR-luminescence, but not for green Tb^{3+}- and red Eu^{3+}-centered luminescence.

Since a ligand-to-metal energy transfer is of great impact in lanthanide-centered luminescence, the ligand-centered emission of Gd^{3+} complexes with ligands **3** and **4** (Fig. 7b) should correlate with the experimentally observed sensitizing effects of the ligands on the emission of their lanthanide complexes (Fig. 7a, c and d). The data (Fig. 7b) reveal similar bands at 480–490 nm, while the emission of the Gd(III) complex with **5** is characterized by a band at shorter wavelengths (~420 nm). A shoulder at the shorter wavelengths is also revealed for the Gd(III) complex with **4**. The emission at 480–500 nm tends to enhance under the longer delay time (Fig. S3 in the ESI†). The decay measurements at 475–500 nm reveal rather long excited state lifetimes (3.5–4.0 μs), which confirms the triplet derived emission at these wavelengths. The phosphorescence emission at 480–500 nm is in good confirmation with the literature results on triplet level energies measured at 77 K for benzoyl-substituted 1,3-diketonate Gd(III) complexes.[53] The emission at 400–430 nm characterized by the excited lifetime in the range of 3.2–3.3 μs should be assigned to 1,3-diketone derived emission.[52] Thus, the data presented in Fig. 7b indicate the great contribution of the 1,3-diketone form for the complexes with ligand **5**, and the small or negligible contributions of its enol forms complexed with Gd(III). This spectral behavior of the complex with **5** is in good agreement with the above mentioned incomplete complex formation of this ligand. It is also worth noting that the spectral behavior of Gd(III) complexes with **3** and **4** reveals them both as better antennae for red Eu^{3+}- and infra-red Yb^{3+}-centered luminescence *versus* green Tb^{3+}-centered emission. Thus, the poor Eu^{3+}-centered luminescence (Fig. 7c) points to efficient quenching processes peculiar for Eu(III) complexes.[54] Moreover, both Tb^{3+}- and Yb^{3+}-centered luminescence (Fig. 7a and d) reveal the difference between ligands **3** and **4**, which indicates that further studies are required to reveal the reasons for the difference.

3. Conclusions

The present work represents the synthesis of novel bis-1,3-diketone derivatives of calix[4]arene with (acetylaceton-3-yl)methyl-, (benzoylaceton-3-yl)methyl- and (dibenzoylmethan-3-yl)methyl-moieties as promising ligands for complex formation with lanthanide ions. The pH-dependent extraction of metal ions at the water–$CHCl_3$ interface indicates efficient complex formation of differently substituted ligands with metal ions, including lanthanides under the equilibrium conditions, while no difference in complex formation with lanthanides is revealed for differently substituted ligands under these conditions.

The great difference between the ligands is revealed from their complex formation with Tb(III) ions in alkaline DMF solutions. The difference results from the retardation of keto–enol transformation in the series of studied calix[4]arenes, which results from bulky β-substituents for the α-substituted 1,3-diketones. In particular, efficient complex formation with Tb^{3+} ions with quick equilibration is observed for the bis-(acetylaceton-3-yl)methyl-acetylacetonate derivative of calix[4]arene in DMF. The substitution of one or two methyl groups in 1,3-diketone fragments by phenyl ones significantly increases the time for the establishment of equilibrium conditions. The Job plot analysis revealed 1 : 1 complex stoichiometry accompanied by the deprotonation of both the 1,3-diketone groups for the ligands under the equilibrium conditions. The quantum-chemical calculations (Sparkle/PM7) point to the cone conformation of calix[4]arene as the most stable one for both free ligand **3** and its deprotonated forms in the Tb^{3+}complexes.

The photophysical properties of the complexes with Tb^{3+}, Eu^{3+}, Yb^{3+} and Gd^{3+} were analyzed with the aim of revealing sensitizing effects of the ligands. The calix[4]arene disubstituted by (acetylaceton-3-yl)methyl-moieties is highlighted for its better antenna effect on Tb^{3+} centered luminescence than the tetra-substituted counterpart. The ligand-centered emission of Gd^{3+} complexes with (benzoylaceton-3-yl)methyl- and (acetylaceton-3-yl)methyl-substituted calix[4]arenes reveals them both as more convenient antennae for red and infra-red than for green lanthanide luminescence, while the data on the (dibenzoylmethan-3-yl)methyl-substituted ligand confirm its incomplete complex formation with lanthanides. Nevertheless, Yb^{3+}-centered luminescence is sensitized to a better extent by a benzoyl-substituted ligand *versus* its acetyl-substituted counterpart, while Tb^{3+} luminescence is sensitized by an acetyl-substituted ligand, not by its benzoyl-substituted counterpart. Moreover, only poor red Eu^{3+} emission is observed under sensitization by both ligands.

Thus, the observed tendency points to the importance of quenching mechanisms along with ligand-to-metal energy transfer on lanthanide-centered luminescence in the complexes with (benzoylaceton-3-yl)methyl- and (acetylaceton-3-yl)methyl-substituted calix[4]arenes.

4. Experimental section

4.1. Reagents and materials

Acetylacetone was distilled before use. 1,4-Dioxane and toluene were purified by distillation over metallic sodium. *N*,*N*-Dimethylformamide (DMF) (Acros Organics) was distilled over P_2O_5. $CDCl_3$ (99.8% isotopic purity) from Aldrich was used for NMR spectroscopy. Terbium nitrate ($Tb(NO_3)_3{\cdot}xH_2O$) (Alfa Aesar), europium nitrate $Eu(NO_3)_3{\cdot}6H_2O$ and triethylamine (TEA) (Acros Organics), neodymium(III) nitrate hexahydrate ($Nd(NO_3)_3{\cdot}6H_2O$) (Aldrich), copper(II) chloride dehydrate ($CuCl_2 2H_2O$), nickel(II) chloride hexahydrate ($NiCl_2 6H_2O$) and aluminum(III) chloride hexahydrate ($AlCl_3 6H_2O$) (Fluca) were used as commercially received without further purification. Stock solutions of metal ions were prepared by dissolving salts in deionized water. All these solutions were standardized by titration using EDTA solution. HI-7004L/C pH 4.01 buffer solution (HANNA), Mes (2-(*N*-morpholino)ethanesulfonicacid (Sigma-Aldrich) and Tris (tris(hydroxymethyl)aminomethane) (Sigma-Aldrich) were used for pH 4.0, pH 5.0–7.0 and pH 8.0, respectively.

4.2. Synthesis

4.2.1. General remarks. The synthetic routes, structural formulae and numbering of atoms of the investigated compounds are shown in Scheme 1. The calix[4]arene **1**[40] and 1,3-diketone **7**[55] were obtained as described in the literature. The synthesis of 5,17-bis(bromomethyl) derivative **2** has been performed by applying a slightly modified procedure.[33] The sodium salt of acetylacetone (NaAA) was synthesized by the addition of an excess of Na (metal plates) to the acetylacetone in absolute toluene. After stirring the mixture at 50 °C for 4 h, the precipitate was decanted from the residues of unreacted sodium, washed with diethyl ether, and dried *in vacuo* at 80 °C for 1 hour. $T_{decomp}{\cdot}$(NaAA) > 198 °C. The sodium salts of 1-benzoylacetone (NaBA) and dibenzoylmethane (NaDBM) were prepared in a similar manner applying equimolar amounts of NaH (60%). $T_{decomp}{\cdot}$(NaBA) > 194 °C and $T_{decomp}{\cdot}$(NaDBM) > 240 °C.

4.2.2. 5,17-Bis[(acetylaceton-3-yl)methyl)]-25,26,27,28-tetrahydroxy-calix[4]arene (3). To a solution of 5,17-bis-(bromomethyl)-25,26,27,28-tetrahydroxycalix[4]arene **2** (1.0 g, 1.64 mmol) in anhydrous dioxane (100 mL), NaAA (0.81g, 6.55 mmol) was added under stirring. The addition of Na salt to the reaction mixture was accompanied (~0.5 h) by an intense pink-violet color which gradually changed to brownish yellow. After stirring the reaction mixture at room temperature for 1 day, the dioxane was distilled off under reduced pressure. The residue was acidified by 1 M HCl (100 mL) and diluted with CH_2Cl_2 (100 mL). The mixture was vigorously stirred until a clear solution formed. The organic layer was separated, washed three times with water, dried over $MgSO_4$ and concentrated by distillation at 80 °C *in vacuo*. The crude product was dissolved in a minor amount of benzene and then precipitated by the hexane. After trituration in hexane and evaporation of solvent, the target product **3** was obtained as a straw colored powder (0.55 g) with a yield of 52%. Mp. 164–165 °C. IR (nujol, cm^{-1}): ν = 3193 (vbr, ν(OH)), 1726, 1699 (ν(C=O)), 1605 (ν(C=O) and ν(C=C)), 1463 (ν(Ph)), 1377, 1358, 1245, 1225, 1150 (ν_{as}(CCC)), 953 (ν_s(CCC)). Anal. calcd for $C_{40}H_{40}O_8$ (648.74): C, 74.06; H, 6.21. Found: C, 73.88; H, 6.15. Mass spectrum (MALDI-TOF): *m*/*z* = 649.3 $[M + H]^+$, 671.2 $[M + Na]^+$.

4.2.3. 5,17-Bis[(benzoylaceton-3-yl)methyl)]-25,26,27,28-tetrahydroxy-calix[4]arene (4). To a solution of 5,17-bis-(bromomethyl)-25,26,27,28-tetrahydroxycalix[4]arene **2** (0.61 g, 1 mmol) in anhydrous dioxane (50 mL), NaBA (0.41 g, 2.2 mmol) was added. The mixture was vigorously stirred. The addition of Na salt (~0.5 h) to the reaction mixture resulted in the appearance of a deep pink-violet color which gradually changed to brownish yellow, similarly to the case with compound **3**. After stirring the reaction mixture at room temperature for 2 days, dioxane was distilled off under reduced pressure. The residue was acidified by 1 M HCl (50 mL) and diluted with CH_2Cl_2 (50 mL). The mixture was vigorously stirred until a clear solution formed. The organic layer was separated, washed several times with water, dried over $MgSO_4$ and concentrated by distillation. Solvent residues were removed at 80 °C *in vacuo*. Thereafter, the crude product was stirred in EtOH (20 mL) at 60 °C for half an hour. The matured precipitate was filtered off and dried under reduced pressure at 80 °C. The target product **4** was obtained (0.47 g) with a yield of 60%. Mp. 148–150 °C. IR (nujol, cm^{-1}): ν = 3167 (vbr, ν(OH)), 1720, 1674 (ν(C=O)), 1596, 1580 (ν(C=O) and ν(C=C)), 1464 (ν(Ph)), 1377, 1358, 1247, 1222, 1152 (ν_{as}(CCC)), 1077, 970 (ν_s(CCC)). Anal. calcd for $C_{50}H_{44}O_8$ (772.88): C, 77.70; H, 5.74. Found: C, 77.88; H, 6.02. Mass spectrum (MALDI-TOF): *m*/*z* = 773.3 $[M + H]^+$, 795.3 $[M + Na]^+$.

4.2.4. 5,17-Bis[(dibenzoylmethan-3-yl)methyl)]-25,26,27,28-tetrahydroxy-calix[4]arene (5). Compound **5** was prepared similarly to compound **3** using NaDBA (0.55g, 2.2 mmol). The target product **5** was obtained (0.5 g) with a yield of 55%. Mp. 140–142 °C. IR (nujol, cm^{-1}): ν = 3160 (vbr, ν(OH)), 1697, 1668 (ν(C=O)), 1596, 1580 (ν(C=O) and ν(C=C)), 1465, 1449 (ν(Ph)), 1377, 1340, 1268, 1229, 1199, 1180 (ν_{as}(CCC)), 1077, 942 (ν_s(CCC)). Anal. calcd for $C_{60}H_{48}O_8$ (897.02): C, 80.34; H, 5.39. Found: C, 80.48; H, 5.15. Mass spectrum (MALDI-TOF): *m*/*z* = 897.3 $[M + H]^+$, 919.3 $[M + Na]^+$.

4.3. Methods

4.3.1. General remarks. Microanalyses of C and H were carried out using a EuroVector CHNS-O Elemental Analyser EA3000. The melting points of the compounds were measured using a Boetius hotstage apparatus. MALDI mass spectra were detected on a Bruker Ultraflex III MALDI-TOF/TOF mass spectrometer. NMR experiments were performed on a Bruker AVANCE-600 spectrometer at 303 K equipped with a 5 mm diameter broadband probe head working at 600.13 MHz in ^{1}H and 150.864 MHz in ^{13}C experiments. Chemical shifts in the ^{1}H and ^{13}C spectra were reported relative to the solvent as an internal standard ($CDCl_3$ $\delta(^1H)$ 7.27 ppm, $\delta(^{13}C)$ 77.2 ppm).

Assignment of signals of the NMR spectra was accomplished by means of 2D COSY, ^{1}H–^{13}C HSQC and ^{1}H–^{13}C HMBC experiments. The pulse programs of the COSY, HSQC and HMBC experiments were taken from Bruker software library. IR absorption spectra were recorded on a Vector-22 Bruker FT-IR spectrophotometer with a resolution of 4 cm^{-1} as Nujol emulsions and KBr pellets of compounds.

UV-VIS absorption spectra have been recorded on a Lambda 35 spectrophotometer (Perkin-Elmer) in 10 mm quartz cuvettes. The Job plotting and spectrometric titration were done from monitoring of absorbance (A_λ).

The steady-state luminescence spectra have been recorded on a spectrofluorometer FL3-221-NIR (Jobin Yvon) with a SPEX FL-1042 phosphorimeter in 10 mm quartz cuvettes. Excitation of the samples was performed at the wavelength values designated in the figure captions and emission detected at 545 nm for Tb(III) with 6/6 nm excitation and emission slits. Time-resolved measurements have been performed on a spectrofluorometer FL3-221-NIR (Jobin Yvon) using the following parameters: time per flash 49.00 ms, flash count 200 ms, initial delay 0.02 ms and sample window 2 ms. The excitation and luminescence spectra of the Gd(III) and Eu(III) complexes were measured with 14/14 nm excitation and emission slits at the wavelength values designated in the figure captions. The Yb(III)-centered excitation and luminescence spectra were measured with 6/6 nm excitation and emission slits at the wavelength values designated in the figure captions.

The time-resolved luminescence spectra and the decay curves were recorded using an optical spectrometer based on an MDR-23 grating monochromator (LOMO, Saint Petersburg, Russia) coupled to a FEU-100 photomultiplier tube.[56] The luminescence was excited by an LGI-21 pulsed nitrogen laser (337 nm wavelength, 2.1 mW laser pulse average output power, 10 ns pulse duration, 100 Hz repetition rate). The average output power of the laser near the samples was 1.7 mW. The exposed surface areas of the samples were 7 mm^2.

All measurements were performed at room temperature under aerated conditions.

4.3.2. Quantum-chemical computations. Structural modeling of the complexes was performed using MOPAC 2012 software.[57] The PM7 semiempirical method was applied by using Sparkle/PM7 Lanthanide Parameters[58] for the Modeling of the Tb(III) complex which allowed computational time and resources to be maximized and the accuracy comparable to non-empirical approaches to be maintained.

4.3.3. Competitive solvent extraction. An aqueous solution (10 mL) containing a mixture of metal salts ([Metal ion] = 0.1 mM) was buffered (50 mM) at pH 4–8 and extracted with a chloroform solution containing a receptor (5.0×10^{-4} M, 10 mL) at 20 °C. HI-7004L/C pH 4.01 buffer solution (HANNA) for pH 4.0, Mes (2-(*N*-morpholino)ethanesulfonic acid) (Sigma-Aldrich) for pH 5.0–7.0 and Tris (tris(hydroxymethyl)aminomethane) (Sigma-Aldrich) for pH 8.0. The mixture was shaken at 230 strokes/min for 24 h. A blank analysis without a receptor was also performed with an aqueous solution of metal salts (0.1 mM, 10.0 mL) and 10.0 mL of chloroform. The residual concentrations of the metal ions determined in the aqueous phase after extraction by compounds **3–5** and after the blank experiments were measured by an atomic emission spectrometer with inductively coupled plasma (ICP-AES, Thermo Scientific, US). The extraction percentage (%*E*) for the metal salts was calculated using the formula %*E* = ([Metal]aq.init − [Metal]aq)/[Metal]aq.init × 100, where ([Metal]aq.init is the concentration of metal ions in the aqueous buffer solution in the blank analysis, and [Metal]aq is the concentration of metal ions remaining in the aqueous solution after their extraction by the investigated ligands. All data were obtained from three independent experiments with a precision of ±3%.

Acknowledgements

This work is supported by the Russian Fund for basic Research (grant 16-03-00007 A). N. Shamsutdinova and G. Gimazetdinova thank the President of Russian Federation grant for young scientists (MK-4456.2015.3) for financial support.

Notes and references

1 A. V. Kel'in and A. Maioli, *Curr. Org. Chem.*, 2003, **7**, 1855–1886.
2 E. A. Shokova, J. K. Kim and V. V. Kovalev, *Russ. J. Org. Chem.*, 2015, **51**(6), 755–830.
3 J. Pradhan and A. Goyal, *Int. J. Pharm. Res. Allied Sci.*, 2015, **4**(2), 1–18.
4 G. G. Condorelli, G. Malandrino and I. L. Fragala, *Coord. Chem. Rev.*, 2007, **251**, 1931–1950.
5 P. A. Vigato, V. Peruzzo and S. Tamburini, *Coord. Chem. Rev.*, 2009, **253**, 1099–1201.
6 K. Binnemans, K. A. Gschneidner Jr., J. C. G. Bünzli and V. K. Pecharsky, *Handbook on the Physics and Chemistry of Rare Earths*, Amsterdam, 2005, ch. 225, vol. 35, pp. 107–272.
7 M. L. P. Reddy, V. Divya and R. Pavithran, *Dalton Trans.*, 2013, **42**, 15249–15262.
8 M. A. Katkova, A. G. Vitukhnovskii and M. N. Bochkarev, *Russ. Chem. Rev.*, 2005, **74**(12), 1089–1109.
9 G. F. de Sá, O. L. Malta, C. de Mello Donegá, A. M. Simas, R. L. Longo, P. A. Santa-Cruz and E. F. da Silva Jr., *Coord. Chem. Rev.*, 2000, **196**, 165–195.
10 J.-C. G. Bunzli and C. Piguet, *Chem. Soc. Rev.*, 2005, **34**, 1048–1077.
11 J.-C. G. Bunzli, *Chem. Rev.*, 2010, **110**, 2729–2755.
12 K. Kuriki, Y. Koike and Y. Okamoto, *Chem. Rev.*, 2002, **102**, 2347–2356.
13 X. H. Wang, H. J. Chang, J. Xie, B. Z. Zhao, B. Liu, S. L. Xua, W. B. Pei, N. Ren, L. Huang and W. Huang, *Coord. Chem. Rev.*, 2014, **273**, 201–212.
14 J.-C. G. Bunzli and S. V. Eliseeva, *Chem. Sci.*, 2013, **4**, 1939–1949.
15 S. V. Eliseeva and J.-C. G. Bunzli, *Chem. Soc. Rev.*, 2010, **39**, 189–227.
16 A. J. Amoroso and S. J. A. Pope, *Chem. Soc. Rev.*, 2015, **44**, 4723–4742.
17 M. C. Heffern, L. M. Matosziuk and T. J. Meade, *Chem. Rev.*, 2014, **114**, 4496–4539.

18 T. Nishioka, J. L. Yuan, Y. J. Yamamoto, K. Sumitomo, Z. Wang, K. Hashino, C. Hosoya, K. Ikawa, G. L. Wang and K. Matsumoto, *Inorg. Chem.*, 2006, **45**(10), 4088–4096.
19 M. Shi, C. Ding, J. Dong, H. Wang, Y. Tian and Z. Hu, *Phys. Chem. Chem. Phys.*, 2009, **11**, 5119–5123.
20 J.-C. G. Bunzli, *Coord. Chem. Rev.*, 2015, **293**, 19–47.
21 C.-J. Xu, B.-G. Li, J.-T. Wan and Z.-Y. Bu, *Spectrochim. Acta, Part A*, 2011, **82**, 159–163.
22 G. Aromí, P. Gamez and J. Reedijk, *Coord. Chem. Rev.*, 2008, **252**, 964–989.
23 J. K. Clegg, S. S. Iremonger, M. J. Hayter, P. D. Southon, R. B. Macquart, M. B. Duriska, P. Jensen, P. Turner, K. A. Jolliffe, C. J. Kepert, G. V. Meehan and L. F. Lindoy, *Angew. Chem., Int. Ed.*, 2010, **49**, 1075–1078.
24 N. A. Shamsutdinova, S. N. Podyachev, S. N. Sudakova, A. R. Mustafina, R. R. Zairov, V. A. Burilov, I. R. Nizameev, I. K. Rizvanov, V. V. Syakaev, B. M. Gabidullin, S. A. Katsuba, A. T. Gubaidullin, G. M. Safiullin and W. Dehaen, *New J. Chem.*, 2014, **38**, 4130–4140.
25 R. Zairov, N. Shamsutdinova, S. Podyachev, S. Sudakova, G. Gimazetdinova, I. Rizvanov, V. Syakaev, V. Babaev, R. Amirov and A. Mustafina, *Tetrahedron*, 2016, **72**, 2447–2455.
26 N. A. Shamsutdinova, A. T. Gubaidullin, B. M. Odintsov, R. J. Larsen, V. D. Schepkin, I. R. Nizameev, R. R. Amirov, R. R. Zairov, S. N. Sudakova, S. N. Podyachev, A. R. Mustafina and A. S. Stepanov, *ChemistrySelect*, 2016, **1**, 1377–1383.
27 N. Shamsutdinova, R. Zairov, A. Mustafina, S. Podyachev, S. Sudakova, I. Nizameev, M. Kadirov and R. Amirov, *Colloids Surf., A*, 2015, **482**, 231–240.
28 R. V. Rodik, A. S. Klymchenko, N. Jain, S. I. Miroshnichenko, L. Richert, V. I. Kalchenko and Y. Mély, *Chem. – Eur. J.*, 2011, **17**, 5526–5538.
29 A. Ikeda and S. Shinkai, *J. Am. Chem. Soc.*, 1994, **116**, 3102–3110.
30 M. H. Düker, R. Gómez, C. M. L. Vande Velde and V. A. Azov, *Tetrahedron Lett.*, 2011, **52**, 2881–2884.
31 M. Strobel, K. Kita-Tokarczyk, A. Taubert, C. Vebert, P. A. Heiney, M. Chami and W. Meier, *Adv. Funct. Mater.*, 2006, **16**, 252–259.
32 T.-D. Guo, Q.-Y. Zheng, L.-M. Yang and Z.-T. Huang, *J. Inclusion Phenom. Macrocyclic Chem.*, 2000, **36**, 327–333.
33 L. O'Toole, J. McGinley and B. S. Creaven, *Tetrahedron*, 2013, **69**, 7220–7226.
34 C. D. Gutsche and K. C. Nam, *J. Am. Chem. Soc.*, 1988, **110**, 6153–6162.
35 M. Almi, A. Arduini, A. Casnati, A. Pochini and R. Ungaro, *Tetrahedron*, 1989, **45**, 2177–2182.
36 L. J. Bellamy, *The Infrared Spectra of Complex Molecules*, Springer Netherlands, 1980.
37 J. Toullec, *The Chemistry of Enols*, Wiley, New York, 1990, vol. 6, pp. 323–398.
38 C. Jaime, J. De Mendoza, P. Prados, P. M. Nieto and C. Sanchez, *J. Org. Chem.*, 1991, **56**, 3372–3376.
39 C. D. Gutsche, J. A. Levine and P. K. Sujeeth, *J. Org. Chem.*, 1985, **50**, 5802–5806.
40 J. Lang, V. Deckerová, J. Czernek and P. Lhoták, *J. Chem. Phys.*, 2005, **122**, 044506.
41 S. N. Podyachev, S. N. Sudakova, A. K. Galiev, A. R. Mustafina, V. V. Syakaev, R. R. Shagidullin, I. Bauer and A. I. Konovalov, *Russ. Chem. Bull.*, 2006, **55**, 2000–2007.
42 N. Iki, N. Morohashi, F. Narumi and S. Miyano, *Bull. Agric. Chem. Soc. Jpn.*, 1998, **71**, 1597–1603.
43 A. V. Kel'in, *Curr. Org. Chem.*, 2003, **7**, 1691–1711.
44 Q. T. H. Le, S. Umetani, M. Suzuki and M. Matsui, J. Chem. Soc., *Dalton Trans.*, 1997, 643–647.
45 D. J. Sardella, D. H. Heinert and B. L. Shapiro, *J. Org. Chem.*, 1969, **34**, 2817–2821.
46 V. Bertolasi, V. Ferretti, P. Gilli, X. Yao and C.-J. Li, *New J. Chem.*, 2008, **32**, 694–704.
47 Y. Suwaa, M. Yamaji and J. of Photochemistry, *J. Photochem. Photobiol., A*, 2016, **316**, 69–74.
48 J. Hong and S. Ham, *Tetrahedron Lett.*, 2008, **49**, 2393–2396.
49 R. J. Bernardino and B. J. Costa Cabral, *J. Phys. Chem. A*, 1999, **103**, 9080–9085.
50 P. Gacoin, *J. Chem. Phys.*, 1972, **57**, 1418–1425.
51 X.-Y. Chen and X. Yang, Bradley J. Holliday, *Inorg. Chem.*, 2010, **49**, 2583–2585.
52 R. E. Whan and G. A. Crosby, *J. Mol. Spectrosc.*, 1962, **8**, 315–327.
53 S. Biju, Y. K. Eom, J.-C. G. Bünzli and H. K. Kim, *J. Mater. Chem. C*, 2013, **1**, 6915–7118.
54 D. D'Alessio, S. Muzzioli, B. W. Skelton, S. Stagni, M. Massi and M. I. Ogden, *Dalton Trans.*, 2012, **41**, 4736.
55 S. N. Podyachev, S. V. Bukharov, I. A. Litvinov, V. I. Morozov, A. T. Gubaidullin, G. N. Nugumanova and N. A. Mukmeneva, *Russ. J. Gen. Chem.*, 2004, **74**, 1775–1781.
56 D. V. Lapaev, V. G. Nikiforov, G. M. Safiullin, I. G. Galyaviev, V. I. Dzabarov, A. A. Knyazev, V. S. Lobkov and Y. G. Galyametdinov, *J. Struct. Chem.*, 2009, **50**, 775–781.
57 J. J. P. Stewart, *MOPAC*, 2012.
58 J. D. L. Dutra, M. A. M. Filho, G. B. Rocha, R. O. Freire, A. M. Simas and J. J. P. Stewart, *J. Chem. Theory Comput.*, 2013, **9**, 3333–3341.